Supplemental Document

Optics EXPRESS

Ab initio spatial phase retrieval via intensity triple correlations: supplement

NOLAN PEARD,[1,2] KARTIK AYYER,[3,4] AND HENRY N. CHAPMAN[2,4,5,6,*]

[1]*Department of Applied Physics, Stanford University, Stanford, CA, USA*
[2]*Center for Free-Electron Laser Science CFEL, Deutsches Elektronen-Synchrotron DESY, Notkestr. 85, 22607 Hamburg, Germany*
[3]*Max Planck Institute for the Structure and Dynamics of Matter, 22761 Hamburg, Germany*
[4]*The Hamburg Center for Ultrafast Imaging, Universität Hamburg, Luruper Chausee 149, 22761 Hamburg, Germany*
[5]*Department of Physics, Universität Hamburg, Luruper Chausee 149, 22761 Hamburg, Germany*
[6]*Department of Physics and Astronomy, Uppsala University, Box 516, Uppsala SE-75120, Sweden*
[*]*henry.chapman@cfel.de*

Supplement DOI: https://doi.org/10.6084/m9.figshare.23617140

Parent Article DOI: https://doi.org/10.1364/OE.495920

Ab Initio Spatial Phase Retrieval via Intensity Triple Correlations: Supplemental Document

1. IMPORTANCE OF THE FOURIER PHASE

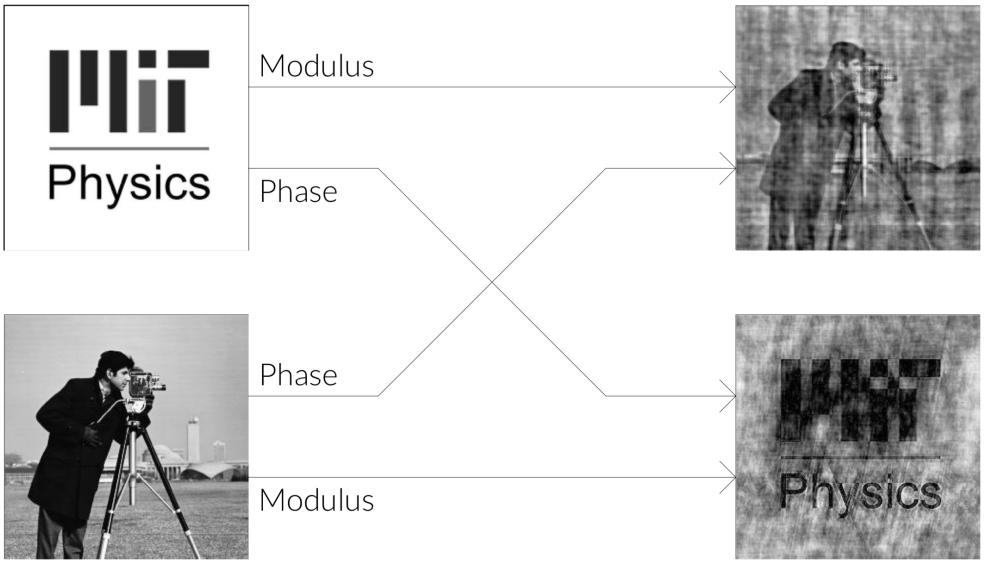

Fig. S1. Two images (left) are Fourier transformed. Swapping the phases of the transformed images and then executing the inverse Fourier transform (right) demonstrates the importance of the phase information in diffractive imaging. Square-law detectors (most photodetectors) cannot access the phase of the light field directly, so creative indirect techniques are required to recover the total light field.

2. DETECTION OF A PHOTON

The reader may wish to refer to [1–4] in the next few sections where we derive the expression for intensity triple correlations used in the main text.

Consider some initial state of the photon field $|i\rangle$ with some detection device in the ground state. $|f\rangle$ is the final state of the field after our detection system has been excited by a photon. The transition amplitude for this event is then

$$A = \langle f | \hat{\psi} | i \rangle \tag{S1}$$

and the transition probability is

$$P = |A|^2 = \left| \langle f | \hat{\psi} | i \rangle \right|^2 \tag{S2}$$

where ψ is the photon field annihilation operator. The final state of the field is usually not observed directly, so we trace over the possible $|f\rangle$

$$P = \sum_f \langle i | \hat{\psi}^\dagger | f \rangle \langle f | \hat{\psi} | i \rangle = \langle i | \hat{\psi}^\dagger \hat{\psi} | i \rangle \tag{S3}$$

This short calculation shows how photon detection is analogous to a measurement of the degree of first-order coherence.

3. FIRST-ORDER COHERENCE IN DIFFRACTION

In coherent diffraction experiments, we measure the degree of first-order coherence as a function of reciprocal space coordinates.

$$G^{(1)}(\vec{k},\vec{k}_0) = \langle \hat{\Psi}^\dagger(\vec{k})\hat{\Psi}(\vec{k}_0)\rangle \tag{S4}$$

where $\hat{\Psi}(\vec{k}) = \sum_i^\nu e^{-i\vec{k}\cdot\vec{r}_i}\hat{a}_i$ is the photon field operator summing over the number of scatterers (ν).

$$G^{(1)}(\vec{k},\vec{k}_0) = \sum_{ij}^{\nu} e^{i\vec{k}\cdot\vec{r}_j}e^{-i\vec{k}_0\cdot\vec{r}_i}\langle \hat{a}_j^\dagger \hat{a}_i\rangle \delta_{ij} \tag{S5}$$

In this picture of elastic scattering, a photon in mode $\vec{k}_0$ is destroyed at site $\vec{r}_i$ and a new photon of the same energy is created in the mode $\vec{k}$ at site $\vec{r}_j = \vec{r}_i$. If we define the momentum transfer vector $\vec{q} = \vec{k} - \vec{k}_0$, then

$$G^{(1)}(\vec{q}) = G^{(1)}(\vec{k},\vec{k}_0) = \sum_{i}^{\nu} e^{i\vec{q}\cdot\vec{r}_i}\langle \hat{a}_i^\dagger \hat{a}_i\rangle \tag{S6}$$

For elastic scattering, we can generally regard the state of the light field to be classical. Furthermore, we consider a system with only one atomic species such that $\alpha_i = \alpha_j = \alpha$, and

$$G^{(1)}(\vec{q}) = |\alpha|^2 \sum_{i}^{\nu} e^{i\vec{q}\cdot\vec{r}_i} \tag{S7}$$

It follows that $G(\vec{0}) = |\alpha|^2 \nu$ so the normalized correlation function is

$$g^{(1)}(\vec{q}) = \frac{G^{(1)}(\vec{q})}{G^{(1)}(\vec{0})} = \frac{1}{\nu}\sum_{k}^{\nu} e^{i\vec{q}\cdot\vec{r}_k} \tag{S8}$$

Photodetectors measure only the fringe visibility (the light intensity), eliminating the phase information of the first-order coherence

$$\left|g^{(1)}(\vec{q})\right| = \frac{1}{\nu}\left|\sum_{k}^{\nu} e^{i\vec{q}\cdot\vec{r}_k}\right| \tag{S9}$$

4. PAIR CORRELATION FUNCTION

Light with no first-order coherence (e.g., fluorescence) can still exhibit second-order coherence. The pair-wise correlation function is written in second-quantization as

$$G^{(2)}(\vec{k}_1,\vec{k}_2) = \langle \hat{\psi}^\dagger(\vec{k}_1)\hat{\psi}^\dagger(\vec{k}_2)\hat{\psi}(\vec{k}_1)\hat{\psi}(\vec{k}_2)\rangle \tag{S10}$$

where the angle brackets indicate the expectation value of a quantum state. Expanding single-particle states in a single mode of momentum-space

$$\hat{\psi}(\vec{k}) = \sum_{i}^{\nu} e^{-i\vec{k}\cdot\vec{r}_i}e^{-i\phi_i}\hat{a}_i = \sum_{i}^{\nu}\mathcal{E}_i(\vec{k})\hat{a}_i \tag{S11}$$

with $\phi_i \in [0, 2\pi)$ a random phase that varies slower than the coherence time. In this picture, each atom at $\vec{r}_i$ emits a photon into the mode $\vec{k}$ with phase ϕ_i.

The pair-wise correlation averaged over an ensemble of measurements (shots) is

$$\left\{G^{(2)}(\vec{k}_1,\vec{k}_2)\right\} = \left\{\sum_{ijkl}^{\nu}\mathcal{E}_i^*(\vec{k}_1)\mathcal{E}_j^*(\vec{k}_2)\mathcal{E}_k(\vec{k}_1)\mathcal{E}_l(\vec{k}_2)\langle \hat{a}_i^\dagger\hat{a}_j^\dagger\hat{a}_k\hat{a}_l\rangle\right\} \tag{S12}$$

The outer braces notate the ensemble mean.

There are two cases where the ensemble mean pair-wise correlation is non-zero:

$$i = k, \quad j = l \tag{S13}$$

$$i = l, \quad j = k \tag{S14}$$

We contract the fields accordingly and rewrite the correlation function as

$$\left\{G^{(2)}(\vec{k}_1,\vec{k}_2)\right\} = \left\{\sum_{ij}^{\nu}\mathcal{E}_i^*(\vec{k}_1)\mathcal{E}_j^*(\vec{k}_2)\mathcal{E}_i(\vec{k}_1)\mathcal{E}_j(\vec{k}_2)\langle\hat{a}_i^\dagger\hat{a}_j^\dagger\hat{a}_i\hat{a}_j\rangle + \mathcal{E}_i^*(\vec{k}_1)\mathcal{E}_j^*(\vec{k}_2)\mathcal{E}_j(\vec{k}_1)\mathcal{E}_i(\vec{k}_2)\langle\hat{a}_i^\dagger\hat{a}_j^\dagger\hat{a}_j\hat{a}_i\rangle - \sum_{i}^{\nu}\mathcal{E}_i^*(\vec{k}_1)\mathcal{E}_i^*(\vec{k}_2)\mathcal{E}_i(\vec{k}_1)\mathcal{E}_i(\vec{k}_2)\langle\hat{a}_i^\dagger\hat{a}_i^\dagger\hat{a}_i\hat{a}_i\rangle\right\} \tag{S15}$$

By writing out the first two terms with i, j indices over the number of emitters we double count the case that $i = j$. In Equation S15, we have subtracted this case once in the last term.

The quantum-classical correspondence between field annihilation/creation operators and classical waves ($\hat{A}^{(+)} \leftrightarrow V$ and $\hat{A}^{(-)} \leftrightarrow V^*$) with normal ordered correlation functions is implemented with the use of the coherent states $|\{\alpha\}\rangle$ [4]. Fock states have no corresponding classical state and must be treated separately.

A. Classical Light

Consider the case that each atom emits a single coherent field so that the initial state of the field is

$$|\{\alpha\}\rangle = \prod_{\lambda}^{\nu}|\alpha_\lambda\rangle \tag{S16}$$

$$\hat{a}_\sigma|\{\alpha\}\rangle = \alpha_\sigma|\{\alpha\}\rangle \tag{S17}$$

where $|\alpha_\lambda\rangle$ is the state contributed by the λth atom. Note that

$$\langle\{\alpha\}|\hat{a}_\mu^\dagger\hat{a}_\sigma|\{\alpha\}\rangle = \alpha_\mu^*\alpha_\sigma \tag{S18}$$

since the coherent states are eigenstates of $\hat{a}$. Because the correlation function operator is normal ordered, we can directly resume from Equation S15 with

$$\left\{G^{(2)}(\vec{k}_1,\vec{k}_2)\right\} = \left\{\sum_{ij}^{\nu}\mathcal{E}_i^*(\vec{k}_1)\mathcal{E}_j^*(\vec{k}_2)\mathcal{E}_i(\vec{k}_1)\mathcal{E}_j(\vec{k}_2)\,|\alpha_i|^2\left|\alpha_j\right|^2 + \mathcal{E}_i^*(\vec{k}_1)\mathcal{E}_j^*(\vec{k}_2)\mathcal{E}_j(\vec{k}_1)\mathcal{E}_i(\vec{k}_2)\,|\alpha_i|^2\left|\alpha_j\right|^2 - \sum_{i}^{\nu}\mathcal{E}_i^*(\vec{k}_1)\mathcal{E}_i^*(\vec{k}_2)\mathcal{E}_i(\vec{k}_1)\mathcal{E}_i(\vec{k}_2)\,|\alpha_i|^4\right\} \tag{S19}$$

Now, the ensemble cancellation of random phases in the $\mathcal{E}_i(k)$ gives the following approximation

$$N\left\{G^{(2)}(\vec{k}_1,\vec{k}_2)\right\} \approx \sum_{ij}^{\nu}\left|\mathcal{E}_i(\vec{k}_1)\right|^2\left|\mathcal{E}_j(\vec{k}_2)\right|^2|\alpha_i|^2\left|\alpha_j\right|^2 + \mathcal{E}_i^*(\vec{k}_1)\mathcal{E}_j^*(\vec{k}_2)\mathcal{E}_j(\vec{k}_1)\mathcal{E}_i(\vec{k}_2)\,|\alpha_i|^2\left|\alpha_j\right|^2 - \sum_{i}^{\nu}\left|\mathcal{E}_i(\vec{k}_1)\right|^4|\alpha_i|^4 \tag{S20}$$

Supposing identical emission from each atom, $\alpha_i = \alpha_j = \alpha$, and recalling $|\mathcal{E}_i(k)|^2 = 1$, we can reduce the sums over constant terms

$$N\left\{G^{(2)}(\vec{k}_1,\vec{k}_2)\right\} \approx \nu^2|\alpha|^4 - \nu|\alpha|^4 + \sum_{ij}^{\nu}\mathcal{E}_i^*(\vec{k}_1)\mathcal{E}_j^*(\vec{k}_2)\mathcal{E}_j(\vec{k}_1)\mathcal{E}_i(\vec{k}_2)\,|\alpha|^4 \tag{S21}$$

We can rewrite the last term

$$\sum_{ij}^{\nu}\mathcal{E}_i^*(\vec{k}_1)\mathcal{E}_i(\vec{k}_2)\mathcal{E}_j^*(\vec{k}_2)\mathcal{E}_j(\vec{k}_1) = \sum_{ij}^{\nu}e^{i(\vec{k}_1-\vec{k}_2)\cdot\vec{r}_j}e^{-i(\vec{k}_1-\vec{k}_2)\cdot\vec{r}_i} = \left|\sum_{j}^{\nu}e^{i\vec{q}\cdot\vec{r}_j}\right|^2 \tag{S22}$$

where $\vec{q} = \vec{k}_1 - \vec{k}_2$. Normalizing the entire correlation function by dividing out the square of

$$N\left\{\langle\hat{\psi}^\dagger(\vec{k}_0)\hat{\psi}(\vec{k}_0)\rangle\right\} = N\left\{\sum_{ij}^{\nu} e^{i\vec{k}_0\cdot(\vec{r}_i-\vec{r}_j)}e^{i(\phi_i-\phi_j)}\langle\hat{a}_i^\dagger\hat{a}_j\rangle\right\} \approx \sum_{ij}^{\nu}\langle\hat{a}_i^\dagger\hat{a}_j\rangle\delta_{ij} = \sum_{i}^{\nu}\langle\hat{a}_i^\dagger\hat{a}_i\rangle = \nu\left|\alpha\right|^2 \tag{S23}$$

we can express the normalized second-order correlation function

$$g^{(2)}(\vec{k}_1,\vec{k}_2) = \frac{\left\{G^{(2)}(\vec{k}_1,\vec{k}_2)\right\}}{\left\{\langle\hat{\psi}^\dagger(\vec{k}_0)\hat{\psi}(\vec{k}_0)\rangle\right\}^2} \tag{S24}$$

as

$$g^{(2)}(\vec{k}_1,\vec{k}_2) \approx 1 - \frac{1}{\nu} + \frac{1}{\nu^2}\left|\sum_{j}^{\nu} e^{i\vec{q}\cdot\vec{r}_j}\right|^2 \tag{S25}$$

Observe that the last term is identical to the modulus square first-order correlation function from Equation S9. Apparently, the coherent diffraction pattern is recovered from photon pair correlations of fluorescence speckle intensities.

$$g^{(2)}(\vec{k}_1,\vec{k}_2) \approx 1 - \frac{1}{\nu} + \left|g^{(1)}(\vec{q})\right|^2 \tag{S26}$$

The imperfect cancellation of random phases causes the "phase noise" of Hanbury Brown and Twiss. The more atoms included, the longer random walk in the complex plane requires additional shots to reach the same level of phase noise as with fewer atoms.

B. Quantum Light

Consider the case that each atom emits a single photon so that the initial state of the field is defined

$$\left|\{n\}\right\rangle = \prod_{\lambda}^{\nu}\left|n_\lambda\right\rangle \tag{S27}$$

$$\hat{a}_\sigma\left|\{n\}\right\rangle = \sqrt{n_\sigma}\left|\{n_1, n_2, ..., n_\sigma - 1, n_{\sigma+1}, ...\}\right\rangle \tag{S28}$$

where $\left|n_\lambda\right\rangle$ is the state contributed by the λth atom. Note that

$$\left\langle\{n\}\right|\hat{a}_\mu^\dagger\hat{a}_\sigma\left|\{n\}\right\rangle = \sqrt{n_\mu}\sqrt{n_\sigma}\delta_{\mu\sigma} \tag{S29}$$

requires an exact match of creation and annihilation operator indices to be non-zero, since Fock states form an orthonormal basis and are not eigenstates of $\hat{a}$ or $\hat{a}^\dagger$.

For coherent states, the normal-ordered correlation operator is already diagonalized. For Fock states, this is not so. The commutation relation $[\hat{a}_i, \hat{a}_j^\dagger] = \delta_{ij}$ allows us to diagonalize the cases S13 and S14

$$\langle\hat{a}_i^\dagger\hat{a}_j^\dagger\hat{a}_i\hat{a}_j\rangle = \langle\hat{a}_i^\dagger\hat{a}_i\hat{a}_j^\dagger\hat{a}_j\rangle - \langle\hat{a}_i^\dagger\hat{a}_j\delta_{ij}\rangle \tag{S30}$$

$$\langle\hat{a}_i^\dagger\hat{a}_j^\dagger\hat{a}_j\hat{a}_i\rangle = \langle\hat{a}_j^\dagger\hat{a}_j\hat{a}_i^\dagger\hat{a}_i\rangle - \langle\hat{a}_j^\dagger\hat{a}_i\delta_{ij}\rangle \tag{S31}$$

as well as the double-counting correction term in S15

$$\langle\hat{a}_i^\dagger\hat{a}_i^\dagger\hat{a}_i\hat{a}_i\rangle = \langle\hat{a}_i^\dagger\hat{a}_i\hat{a}_i^\dagger\hat{a}_i\rangle - \langle\hat{a}_i^\dagger\hat{a}_i\rangle \tag{S32}$$

Writing the expectation value $\langle\hat{a}_i^\dagger\hat{a}_i\rangle = n_i$ as the occupation number of the mode emitted by the ith atom, the diagonalized second order correlation function (Eq. S15) reads

$$\left\{G^{(2)}(\vec{k}_1,\vec{k}_2)\right\} = \left\{\sum_{ij}^{\nu} n_i n_j\left|\mathcal{E}_i(\vec{k}_1)\right|^2\left|\mathcal{E}_j(\vec{k}_2)\right|^2 + n_i n_j\mathcal{E}_i^*(\vec{k}_1)\mathcal{E}_i(\vec{k}_2)\mathcal{E}_j^*(\vec{k}_2)\mathcal{E}_j(\vec{k}_1) - \sum_{i}^{\nu} n_i^2\left|\mathcal{E}_i(\vec{k}_1)\right|^4 - \sum_{i}^{\nu} n_i\left|\mathcal{E}_i(\vec{k}_1)\right|^4\right\} \tag{S33}$$

Supposing single photon emission from identical atoms, $n_i = n_j = 1$ and writing $\left|\mathcal{E}_j(k_2)\right|^2 = 1$, we get

$$\left\{G^{(2)}(\vec{k}_1,\vec{k}_2)\right\} = \left\{\nu^2 - 2\nu + \sum_{ij}^{\nu} \mathcal{E}_i^*(\vec{k}_1)\mathcal{E}_i(\vec{k}_2)\mathcal{E}_j^*(\vec{k}_2)\mathcal{E}_j(\vec{k}_1)\right\} \tag{S34}$$

Normalizing by $\left\{\hat{\psi}^\dagger(\vec{k}_0)\hat{\psi}(\vec{k}_0)\right\}^2 = \nu^2$ as in the previous section, we obtain

$$g^{(2)}(\vec{k}_1,\vec{k}_2) = 1 - \frac{2}{\nu} + \left|g^{(1)}(\vec{q})\right|^2 \tag{S35}$$

which is quite similar to the case where we assume classical light. Note here, however, that the expression is an exact equality - this is due to the orthogonality of Fock states contracting only those random phases which cancel perfectly. There are no $\left\{e^{i\phi_i}e^{-i\phi_j}\right\}$ terms where $i \neq j$, so the ensemble average over shots is not subject to the Hanbury Brown and Twiss phase noise.

5. TRIPLE CORRELATION FUNCTION

The correlation function between triples of photons is written in second-quantization as

$$G^{(3)}(\vec{k}_1,\vec{k}_2,\vec{k}_3) = \langle\hat{\psi}^\dagger(\vec{k}_1)\hat{\psi}^\dagger(\vec{k}_2)\hat{\psi}^\dagger(\vec{k}_3)\hat{\psi}(\vec{k}_1)\hat{\psi}(\vec{k}_2)\hat{\psi}(\vec{k}_3)\rangle \tag{S36}$$

where the field operators are defined as before. The triple correlation averaged over an ensemble of measurements is

$$\left\{G^{(3)}(\vec{k}_1,\vec{k}_2,\vec{k}_3)\right\} = \left\{\sum_{ijklmn}^{\nu} \mathcal{E}_i^*(\vec{k}_1)\mathcal{E}_j^*(\vec{k}_2)\mathcal{E}_k^*(\vec{k}_3)\mathcal{E}_l(\vec{k}_1)\mathcal{E}_m(\vec{k}_2)\mathcal{E}_n(\vec{k}_3)\langle\hat{a}_i^\dagger\hat{a}_j^\dagger\hat{a}_k^\dagger\hat{a}_l\hat{a}_m\hat{a}_n\rangle\right\} \tag{S37}$$

and again we must consider the field contractions for which the expression is non-zero. We find that there are six

$$i = l, \quad j = m, \quad k = n \tag{S38}$$
$$i = n, \quad j = l, \quad k = m \tag{S39}$$
$$i = m, \quad j = n, \quad k = l \tag{S40}$$
$$i = l, \quad j = n, \quad k = m \tag{S41}$$
$$i = n, \quad j = m, \quad k = l \tag{S42}$$
$$i = m, \quad j = l, \quad k = n \tag{S43}$$

The first case (S38) contracts fields with the same $\vec{k}$, and will thus be a constant after summation and averaging. For the remaining cases, we must carefully account for double- and triple-counting. We can quickly see that cases S41, S42, and S43 each contract one set of fields with the same $\vec{k}$, leaving a pair of free indices which do not contract to a constant. Each of these pairs over count S38 when the indices are equal, so we must subtract this case from each of S41, S42, and S43. The cases S39 and S40, however, have three free indices which do not produce field contractions to a constant. Firstly, we can contract any pair of the three indices in each of S39 and S40 to get the result of any one of S41, S42, and S43 again - this over counts each of S41, S42, and S43 once for each of S39 and S40. Additionally, this overcounting correction must itself be corrected just as S41, S42, and S43 were above. Finally, S39 and S40 each overcount the case where all three indices

are equal. All cases (S38 through S43) over-counting corrections can be expressed as

$$\begin{aligned}
&\delta_{il}\delta_{jm}\delta_{kn} \\
&+\delta_{in}\delta_{jl}\delta_{km}\left(1-\delta_{ij}\right)\left(1-\delta_{jk}\right)\left(1-\delta_{ki}\right) \\
&+\delta_{im}\delta_{jn}\delta_{kl}\left(1-\delta_{ij}\right)\left(1-\delta_{jk}\right)\left(1-\delta_{ki}\right) \\
&+\delta_{il}\delta_{jn}\delta_{km}\left(1-\delta_{jk}\right) \\
&+\delta_{in}\delta_{jm}\delta_{kl}\left(1-\delta_{ki}\right) \\
&+\delta_{im}\delta_{jl}\delta_{kn}\left(1-\delta_{ij}\right) \\
&=\delta_{il}\delta_{jm}\delta_{kn} \\
&+\delta_{in}\delta_{jl}\delta_{km}(1-\delta_{ij}-\delta_{jk}-\delta_{ki}+\delta_{ij}\delta_{jk}+\delta_{jk}\delta_{ki}+\delta_{ki}\delta_{ij}-\delta_{ij}\delta_{jk}\delta_{ki}) \\
&+\delta_{im}\delta_{jn}\delta_{kl}(1-\delta_{ij}-\delta_{jk}-\delta_{ki}+\delta_{ij}\delta_{jk}+\delta_{jk}\delta_{ki}+\delta_{ki}\delta_{ij}-\delta_{ij}\delta_{jk}\delta_{ki}) \\
&+\delta_{il}\delta_{jn}\delta_{km}\left(1-\delta_{jk}\right) \\
&+\delta_{in}\delta_{jm}\delta_{kl}\left(1-\delta_{ki}\right) \\
&+\delta_{im}\delta_{jl}\delta_{kn}\left(1-\delta_{ij}\right)
\end{aligned} \tag{S44}$$

when contracted with the six-fold sum S37.

A. Classical Light

Consider once more our scenario where classical light is emitted

$$|\{\alpha\}\rangle = \prod_{\lambda}^{\nu} |\alpha_\lambda\rangle \tag{S45}$$

As with the pair correlation operator above, the triple correlation operator is diagonal in the coherent state basis. Proceeding analogously and defining

$$\vec{q}_1 = \vec{k}_1 - \vec{k}_2 \tag{S46}$$

$$\vec{q}_2 = \vec{k}_2 - \vec{k}_3 \tag{S47}$$

$$\vec{q}_3 = \vec{k}_3 - \vec{k}_1 = -\vec{q}_1 - \vec{q}_2 \tag{S48}$$

we soon reach the expression

$$\begin{aligned}
N\left\{G^{(3)}(\vec{k}_1,\vec{k}_2,\vec{k}_3)\right\} \approx &\left(\nu^3-3\nu^2+4\nu\right)|\alpha|^6 \\
&+(\nu-2)\left(\left|\sum_j^{\nu}|\alpha|^3\, e^{i\vec{q}_1\cdot\vec{r}_j}\right|^2+\left|\sum_j^{\nu}|\alpha|^3\, e^{i\vec{q}_2\cdot\vec{r}_j}\right|^2+\left|\sum_j^{\nu}|\alpha|^3\, e^{i\vec{q}_3\cdot\vec{r}_j}\right|^2\right) \\
&+|\alpha|^6\sum_{ijk}e^{i\vec{q}_1\cdot\vec{r}_i}e^{i\vec{q}_2\cdot\vec{r}_j}e^{i\vec{q}_3\cdot\vec{r}_k}+|\alpha|^6\sum_{ijk}e^{-i\vec{q}_1\cdot\vec{r}_i}e^{-i\vec{q}_2\cdot\vec{r}_j}e^{-i\vec{q}_3\cdot\vec{r}_k}
\end{aligned} \tag{S49}$$

remembering the over-counting rules from the previous section. Observe that the last two terms are products of independent sums and complex conjugates. Moreover, each of the second, third, and fourth terms is a first-order correlation function S7. After normalizing by the cube of $|\alpha|^2\,\nu$, we write

$$\begin{aligned}
\left\{g^{(3)}(\vec{k}_1,\vec{k}_2,\vec{k}_3)\right\} \approx &\left(1-\frac{3}{\nu}+\frac{4}{\nu^2}\right)+\left(1-\frac{2}{\nu}\right)\left(\left|g^{(1)}(\vec{q}_1)\right|^2+\left|g^{(1)}(\vec{q}_2)\right|^2+\left|g^{(1)}(\vec{q}_3)\right|^2\right) \\
&+2\mathrm{Re}\left(g^{(1)}(\vec{q}_1)g^{(1)}(\vec{q}_2)g^{(1)}(\vec{q}_3)\right)
\end{aligned} \tag{S50}$$

The last term here is the subject of the main text and allows retrieval of the exact structural phase $\phi(\vec{q})$ sought in coherent diffraction experiments.

B. Quantum Light

As with the pair correlations of quantum light, the triple correlator acting on non-classical states of the field picks up additional corrections during diagonalization. There are six terms (neglecting the over-counting correction terms, which must also be diagonalized) that must be diagonalized in the Fock basis. As an example, diagonalizing the first term of S44 produces the operator

$$\langle \hat{a}_i^\dagger \hat{a}_j^\dagger \hat{a}_k^\dagger \hat{a}_i \hat{a}_j \hat{a}_k \rangle = \langle \hat{a}_i^\dagger \hat{a}_i \hat{a}_j^\dagger \hat{a}_j \hat{a}_k^\dagger \hat{a}_k - \hat{a}_i^\dagger \hat{a}_i \hat{a}_j^\dagger \hat{a}_k \delta_{jk} - \hat{a}_i^\dagger \hat{a}_j \hat{a}_k^\dagger \hat{a}_k \delta_{ij} + \hat{a}_i^\dagger \hat{a}_k \delta_{ij} \delta_{kj} - \hat{a}_i^\dagger \hat{a}_k \hat{a}_j^\dagger \hat{a}_j \delta_{ik} + \hat{a}_i^\dagger \hat{a}_j \delta_{ik} \delta_{jk} \rangle \quad \text{(S51)}$$

Clearly, obtaining the exact form of the triple correlations for chaotic quantum light is a tedious task. The result is not important for this paper, but it is important to realize that the classical and quantum cases lead to different expressions. We will skip this derivation for now.

6. FRIEDEL'S LAW AND SYMMETRIES OF Φ

Given a real function $f(x)$, its Fourier Transform $F(k) = \mathcal{F}(f(x))$ has the following properties:

$$F(k) = F^*(-k) \quad \text{(S52)}$$

$$|F(k)|^2 = |F(-k)|^2 \quad \text{(S53)}$$

For $\phi(k) = \arg(F(k))$,

$$\phi(-k) = -\phi(k) \quad \text{(S54)}$$

leads to some useful symmetries of the correlation functions and phase map

$$g^{(1)}(x) = g^{(1)*}(-x) \quad \text{(S55)}$$

$$\Phi(m,n) = \Phi(n,m) \quad \text{(S56)}$$

$$\Phi(0,n) = \Phi(m,0) = 0 \quad \text{(S57)}$$

$$\Phi(m,n) = \Phi(-n,-m) \quad \text{(S58)}$$

$$\Phi(-m,m) = 0 \quad \text{(S59)}$$

7. COHERENT DIFFRACTION PATTERN RETRIEVAL

Fig. S2 shows the result of calculating the pairwise correlation function $g^{(2)}(\vec{q})$ from first-order incoherent fluorescence of atoms. The autocorrelation enables accurate retrieval of the coherent diffraction pattern out to $2|\vec{k}_{\max}|$ (past the physical edge of the detector at $|\vec{k}_{\max}|$) [5].

8. EXTENDED MOMENTUM SPACE SAMPLING ENHANCES REAL SPACE RESOLUTION

Fig. S3 shows that extended sampling of momentum space enhances the resolution of the real space autocorrelation and, if the phase information is available, the resolution of inverse Fourier Transform (the object).

9. THE CROSS-CORRELATION THEOREM

For correlations of one-dimensional or small two-dimensional pixel arrays, computationally, it is usually faster to work directly with the outer product of the arrays, sum the resulting matrix along the diagonal, and divide out the underlying support (which represents correlations of unbunched photons). However, for larger arrays, this computation rapidly becomes memory-limited; for example, the second-order correlation of a typical 1000 by 1000 pixel array involves the calculation of a four-dimensional array represented by 1000^4 floating point numbers. If each floating point number were 32 bits, we would need about 4 terabytes to store this array.

The Cross-Correlation Theorem provides a simple method to calculate correlations using the Fast Fourier Transform. Let $f \bigstar g$ denote the cross correlation of $f(x)$ and $g(x)$. The Cross-Correlation Theorem states

$$f \bigstar g = \mathcal{F}^{-1}[F(k)G^*(k)] \quad \text{(S60)}$$

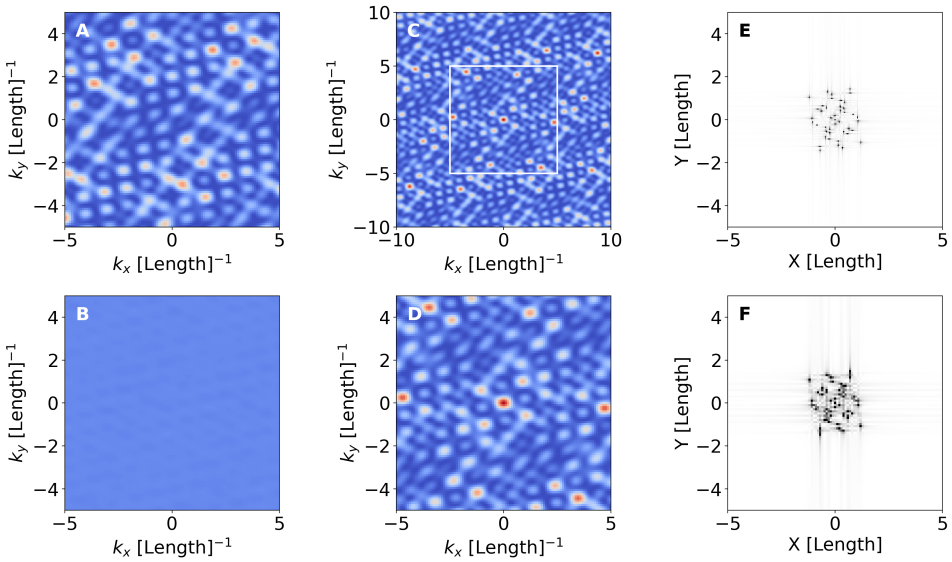

Fig. S2. Simulated fluorescence from a 2D array of seven classical point sources. (A) shows a speckle pattern, representing a single (random) phase relationship between point sources. (B) shows the mean of 1000 speckle patterns with the atom phases changing between shots. The result has nearly zero contrast. The sum of second-order (auto)correlations of the same shots (C) contains the coherent diffraction pattern (D) in the boxed region of (C) plus extra coherent diffraction data beyond the maximum scattering angle covered by the detector. The augmented $\vec{k}$-space window produces a real space (object) autocorrelation function with enhanced spatial resolution (E) compared to the real space autocorrelation (F) obtained from inverse Fourier inversion of (C) and (D).

where $\mathcal{F}^{-1}$ indicates the inverse Fourier transform and $F(k)$ and $G(k)$ are the Fourier transforms of $f(x)$ and $g(x)$. If f and g are real-valued then

$$f \bigstar g = \mathcal{F}^{-1}[F(k)G(-k)] = f(x) * g(-x) \tag{S61}$$

The autocorrelation $G^{(2)}(k_1, k_2)$ of intensities $I(k)$ on a detector is then

$$G^{(2)}(k_1 - k_2) = I(k_1) \bigstar I(k_2) = I(k_1) * I(-k_2) \tag{S62}$$

where the last expression is the convolution of intensities.

The triple correlation

$$G^{(3)}(k_1, k_2, k_3) = I(k_1) \bigstar I(k_2) \bigstar I(k_3) \tag{S63}$$

is most easily calculated from the bispectrum as

$$G^{(3)}(q_1, q_2) = \mathcal{F}^{-1}[\tilde{I}(u)\tilde{I}(v)\tilde{I}(-u - v)] \tag{S64}$$

where $u = k_1 - k_2$ and $v = k_2 - k_3$.

10. COARSE BINNING AND INTERPOLATION OF PHASE INFORMATION

A major difficulty of performing a triple correlation experiment is the computational complexity of the method. For a square, two-dimensional detector with side length of N pixels, the third-order correlation function (correlations between triples of pixels) is a six-dimensional function. This must either be stored in memory or rapidly generated on-the-fly during phase retrieval, neither of which is an attractive option for working with large detectors.

We can consider a case where the sampling rate of the triple correlation may be reduced, the phase retrieved and interpolated, and combined with densely sampled diffraction data. The upscaled phase information breaks the symmetry of the real space structure autocorrelation,

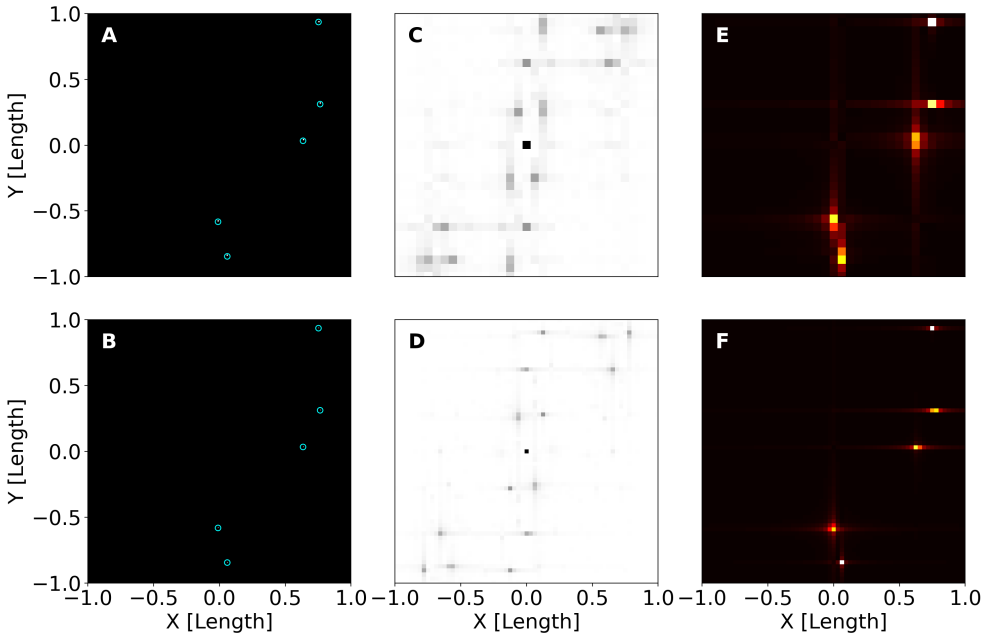

Fig. S3. (A) and (B) show the same array of atoms. (B) has double the spatial resolution (localization) of (A). The inverse Fourier Transform of simulated coherent diffraction (C) and (D) retrieves only the real space autocorrelation of the array since the phase information has been lost. In (E) and (F), the phase information is added back to break the translational symmetry and arrive at the original array. Note that in (D) and (F), where the simulated coherent diffraction goes out to $2\left|\vec{k}_{\max}\right|$, it is possible to resolve nearby atoms with much greater visibility than in (C) and (E), in which only data out to $\left|\vec{k}_{\max}\right|$ in momentum space is used.

selecting peaks at the true atomic positions. For example, Fig. S4 shows that phase information sampled at 30 pixels combined with the modulus from coherent diffraction data sampled at 200 pixels across the same region of $\vec{k}$-space retrieves a noisy, but discernible structure.

11. LINEAR PHASE RAMPS AND SIGN FLIPS SHIFT AND INVERT THE FOURIER TRANSFORM

Fig. S5 demonstrates the effect of linear ramps and sign flips of the phase in real space. A linear phase ramp in momentum space produces a translation in real space. A sign flip of the entire phase inverts the real space structure. Both exact numerical solving and differential evolution structure fitting obtain the phase accurately up to a linear phase ramp or sign flip (or both) in most cases, maintaining the correct relative positions but producing incorrect absolute positions and orientations.

12. HARMONIC INVERSION RESOLVES REAL SPACE POSITIONS FROM FOURIER DATA

In Fig. S5 we used harmonic inversion to retrieve precise real space positions of the atoms from the Fourier modulus and phase. The inverse Fourier transform gives peaks with a finite width and, thus, uncertainty in the position of the atom. Harmonic inversion is not limited by the Fourier uncertainty principle and superresolves the positions of the atoms directly from the momentum space data rather than the Fourier transform [6–8].

13. 1D PHASE RETRIEVAL EXAMPLE

A. Exact Coherent Phase Retrieval

Using Equation 11 and the algorithm described in Section 3, we can calculate the Fourier phase from triple correlation data and compare the result to the true value. Figure S6 shows the results of phase retrieval in a simulation with a 1D pixel detector.

B. Coherent Phase Retrieval via Fitting

Retrieval of the Fourier phase is highly sensitive to statistical and systematic noise. The examples of exact phase retrieval shown in the previous section were calculated for ideal experimental conditions with no sources of noise. Noise is especially problematic in the division step of Equation 11. Moreover, it is expected that the phase noise will become problematic for sources with large numbers of incoherent atoms [5]. Therefore, phase retrieval via an optimization algorithm which compares the closure phase (Equation 12) of a trial atom array to a measured closure phase may be more tractable for real experimental data.

We used a differential evolution algorithm to iterate on the spatial arrangement of the atoms until satisfactory convergence between the simulated closure phase and the closure phase of the trial structure was achieved. It can be seen in Fig. S6 that the exact method based on the algorithm and the structure optimization method achieve similar results.

14. ALTERNATE PHASE TOGGLING

Figure S7 illustrates how phase toggling is implemented in the algorithm from the main text.

REFERENCES

1. R. J. Glauber, "Photon correlations," Phys. Rev. Lett. **10**, 84–86 (1963).
2. R. J. Glauber, "The quantum theory of optical coherence," Phys. Rev. **130**, 2529–2539 (1963).
3. R. J. Glauber, "Coherent and incoherent states of the radiation field," Phys. Rev. **131**, 2766–2788 (1963).
4. J. Peřina, *Quantum Statistics of Linear and Nonlinear Optical Phenomena* (Springer Netherlands, 1991), 2nd ed.
5. F. Trost, K. Ayyer, and H. N. Chapman, "Photon statistics and signal to noise ratio for incoherent diffraction imaging," New J. Phys. **22**, 083070 (2020).
6. V. A. Mandelshtam and H. S. Taylor, "Harmonic inversion of time signals and its applications," The J. Chem. Phys. **107**, 6756–6769 (1997).
7. V. A. Mandelshtam and H. S. Taylor, "Multidimensional harmonic inversion by filter-diagonalization," The J. Chem. Phys. **108**, 9970–9977 (1998).
8. V. A. Mandelshtam, "On harmonic inversion of cross-correlation functions by the filter diagonalization method," J. Theor. Comput. Chem. **02**, 497–505 (2003).

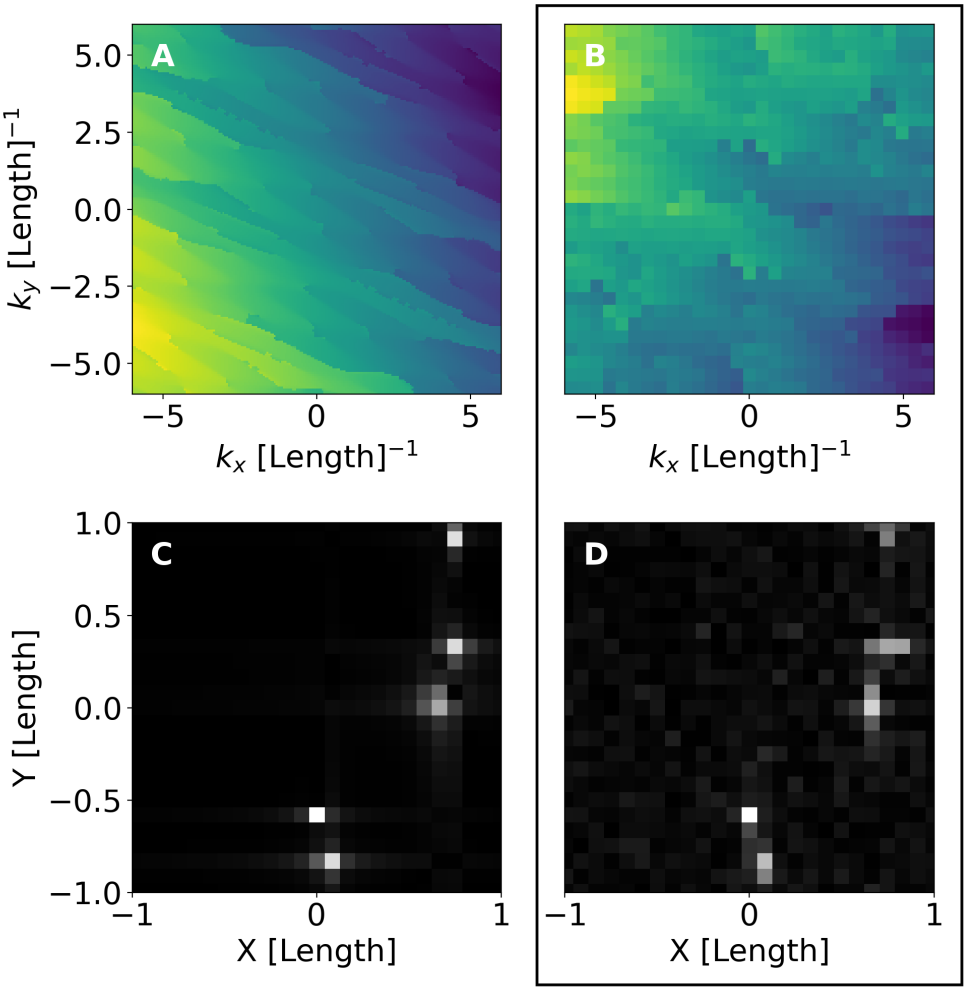

Fig. S4. (A) shows the phase $\phi(\vec{k})$ sampled and unwrapped across 201 by 201 pixels. (B) shows $\phi(\vec{k})$ sampled and unwrapped across 29 by 29 pixels on the same area of $\vec{k}$-space. (C) is the result of taking the inverse Fourier transform using the phase shown in (A). (D) is the result of taking the inverse Fourier transform using the phase in (B) (interpolated to the same sampling resolution as in (A)) and the same modulus used to produce (C). (D) suffers from additional noise compared to (C), but each of the five atoms remains well-resolved.

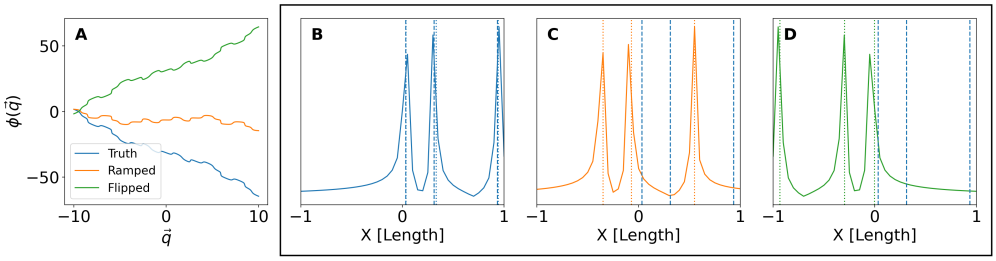

Fig. S5. (A) shows three phases which, combined with identical modulus data, produce different inverse Fourier transforms in (B), (C), and (D). The blue phase (A) and Fourier transform (B) represent the truth values. The orange phase (A) has acquired an additional linear ramp compared to the truth phase which results in a shifted Fourier transform (C) compared to the truth Fourier transform in (B). The green phase (A) has a sign flip with respect to the truth phase, causing the Fourier transform in (D) to appear inverted across the origin. Compounded ramps and sign flips of the phase result in compounded shifts and inversions of the Fourier transform. In each of (B), (C), and (D), the blue vertical dashes mark the truth positions of the atoms used in the model. The vertical dots (color matches color of phase pictured in (A)) indicate the atom positions calculated via harmonic inversion of the modulus and phase. In the case of (B), harmonic inversion determines the truth positions of the atoms quite accurately. In (C) and (D), sub-linewidth positions of the shifted and inverted atom array are shown to maintain the correct interatomic separations. The Fourier transforms (solid curves) are each normalized to the height of the tallest peak.

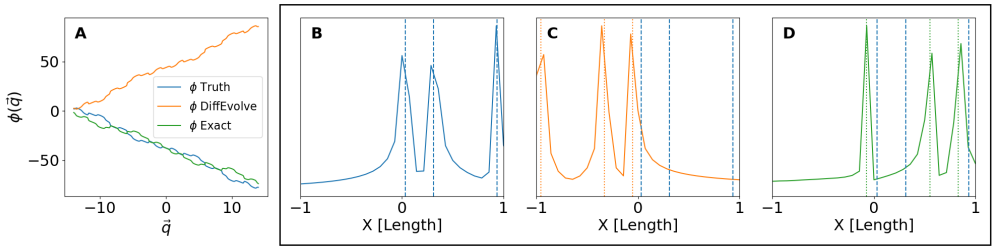

Fig. S6. Phase retrieval results compared to truth values (blue) for a 1D array of three atoms using the exact numerical solution (green) of Section 3 and differential evolution (orange). (A) shows the retrieved (orange and green) and truth (blue) phases used, together with the modulus obtained from Equation 9, to execute the inverse Fourier transform in (B), (C), and (D). In (B), the truth object from the inverse Fourier transform and the known positions (vertical dots) of the atoms match, unsurprisingly. (C) shows that differential evolution correctly found atom positions (orange vertical dots) with the correct separation and ordering, but the structure appears flipped and shifted compared to the truth positions (blue vertical dots). This is due to the linear phase ramp in (A) compared to the truth phase. The effect of linear phase ramps and sign flips is detailed in Supplement 11. Similarly, the exact numerical solution in (D) also retrieved the correct interatomic separations but the phase (green) in (A) is inverted to the truth phase, causing a flip of the real space structure. Since the exact numerical algorithm finds the phase without directly determining atom positions, we used harmonic inversion (see Supplement 12) to determine a sub-linewidth position for the three atoms (green vertical dots) to compare to the truth atom positions (blue vertical dots). The Fourier transforms (solid curves) are each normalized to the height of the tallest peak.

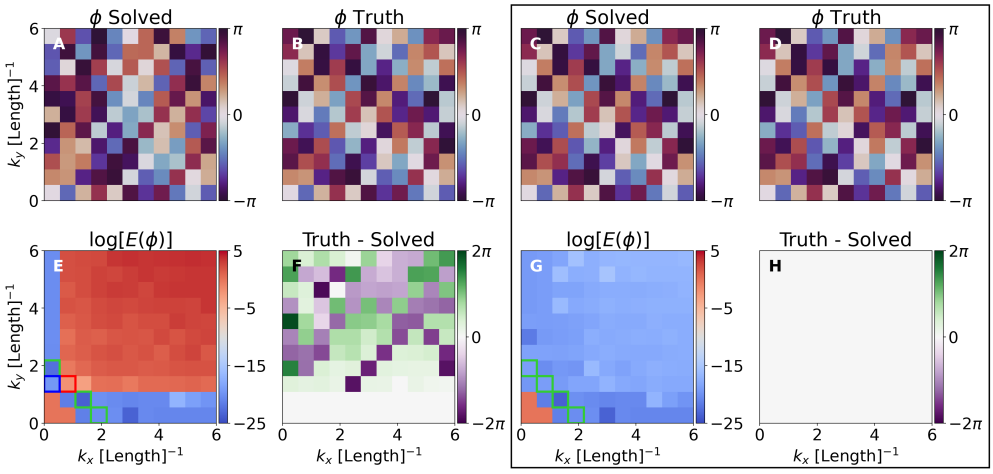

Fig. S7. In these examples, the value of $\phi(\vec{k})$ in (A) and (C) in each diagonal $k_y = -k_x + n$, $n \in \mathbb{Z}$ is determined beginning at the origin and ending in the upper right corner. In the first example (left), where toggling is not used, the solved value of ϕ in (A) has a large difference (F) from the true value of ϕ in (B). We observe that the value of $\log\left[E(\phi)\right]$ (E) is seen to spike (red box) along the third diagonal (green and red boxes). The value of the error function increases and propagates to surrounding pixels as additional diagonals are solved. This indicates that a pixel in the second diagonal (blue box) has been assigned incorrectly. Resolving the second diagonal by substituting alternate minima of $\log\left[E(\phi)\right]$ eventually arrives at a $\phi(\vec{k})$ (C) which has uniformly low values of the error function (G) such that the difference (H) between the solution (C) and truth (D) is quite small. Note that the error function, (E) and (G), is defined to be zero at the origin and the origin nearest neighbors as these values of $\phi(\vec{k})$ are free parameters of the solution process.